

## Electrospun Thermosetting Carbon Nanotube-Epoxy Nanofibers

Nojan Aliahmad<sup>1</sup>, Pias Kumar Biswas<sup>1,2</sup>, Vidya Wable<sup>1,2</sup>, Iran Hernandez<sup>1</sup>, Amanda Siegel<sup>1,3</sup>, Hamid Dalir<sup>1,2,3\*</sup>, and Mangilal Agarwal<sup>1,2,3\*</sup>

<sup>1</sup>Integrated Nanosystems Development Institute (INDI) and <sup>2</sup>Department of Mechanical and Energy Engineering, Indiana University-Purdue University Indianapolis, IN 46202; <sup>3</sup>Multiscale Integrated Technology Solutions LLC, IN 46033.

Correspondence: H. D., [hdalir@iupui.edu](mailto:hdalir@iupui.edu); M. A., [agarwal@iupui.edu](mailto:agarwal@iupui.edu)

### Abstract:

This paper represents the process of fabrication and characterization of submicron carbon nanotubes (CNT)-epoxy nanocomposite filaments through an electrospinning process. Electrospinning is one of the most versatile, inexpensive, and environmentally well-known techniques for producing continuous fibers from submicron diameter all the way to tens of nanometer diameter. Here, electrospinning of submicron epoxy filaments was made possible by partially curing of the epoxy by mixing the hardener and through a thermal treatment process without the need for adding any plasticizers or thermoplastic binders. This semi-curing approach makes the epoxy solution viscous enough for electrospinning process, i.e., without any solidification or non-uniformity caused by the presence of hardener inside the mixture. The filaments were spun using a CNT/epoxy solution with a viscosity of 65p using 16kV and collector distance of 10 cm. The diameter of these filaments can be tuned as low as 100 nm with adjustment of electrospinning parameters. By incorporating a low amount of CNT into epoxy, better structural, electrical, and thermal stability were achieved. The CNT fibers have been aligned inside the epoxy filaments due to the presence of the electrostatic field during the electrospinning process. The modulus of the epoxy and CNT/epoxy filaments were found to be 3.24 and 4.84 GPa, respectively. The presence of CNT can lead up to 49% improvement on modulus. Accordingly using a commercially available epoxy suitable for industrial composite productions makes the developed filament suitable for many applications.

---

This is the author's manuscript of the article published in final edited form as:

Aliahmad, N., Biswas, P. K., Wable, V., Hernandez, I., Siegel, A., Dalir, H., & Agarwal, M. (2021). Electrospun Thermosetting Carbon Nanotube–Epoxy Nanofibers. *ACS Applied Polymer Materials*, 3(2), 610–619. <https://doi.org/10.1021/acsp.0c00519>

**Introduction:**

With the emergence of nanotechnology, researchers all over the world have been extensively devoting efforts to the preparation and discovery of new nanocomposites for various commercial applications<sup>1-4</sup>. The advantage of making these nanocomposites is to achieve better properties such as higher mechanical properties, thermal stability, and efficiency. Nanocomposites can be formed in different shapes such as flakes, fibers and hybrids<sup>5</sup>. Several researches have been conducted to extrude nanofilaments made out of neat thermoplastic epoxy and nanocomposites<sup>6</sup>. Despite the research and progress on making composite-based nanosized filaments, the fabrication of a thermosetting nanocomposite has still remained a challenge. There are several limiting factors of making a continuous filament out of thermosetting epoxy, while the thermosetting polymers are limited to be extruded or stretched. Furthermore, having a uniform nanocomposite by adding nanomaterials to the thermosetting epoxy composite is still a challenge. In this paper, an electrospinning based approach has been developed and tested to overcome the limits of fabricating a nanocomposite thermosetting epoxy filament with diameters in nanoscale range.

Compared to contemporary approaches for fabricating continuous nanofibers, electrospinning, which involves electrohydrodynamic phenomena, is widely acknowledged as the most versatile, effective and economically beneficial process<sup>7</sup>. This simple voltage-driven, electrostatic method only requires a pump, a high voltage power source, a collector and a solution reservoir tipped with a blunt needle<sup>8</sup>. Voltage, flow rate, needle-collector distance, viscosity, and type of solvents all represent key parameters in regulating the properties of the fibers created through electrospinning<sup>9-12</sup>. Different polymers have been examined in the past and have been shown compatible with electrospinning<sup>13</sup>. The uniform polymer nanofibers structures formed by electrospinning have been reported to have diameters ranging from 2 nm to several microns<sup>13</sup> and exhibit superior properties like the high surface area to volume ratio, flexibility in surface functionalities<sup>14</sup>, inter/intra fibrous porosity, and extraordinary mechanical properties.

Thermosetting epoxy nanofibers are gaining tremendous popularity in many structural applications such as interlayer reinforcement in Carbon Fiber Reinforced Polymer (CFRP) composites. However, the production of these fibers at the nanoscale has never been achieved. Nanofibers synthesized via electrospinning of thermoplastic polymers such as Polyaniline (PANI), Polyvinylpyrrolidone (PVP), Polyvinyl alcohol (PVA), Polycaprolactone (PCL), etc<sup>15</sup> have been investigated in the development of thermoset-thermoplastic blending and core-sheath to fabricate such fibers (e.g. Polycaprolactone/Epoxy<sup>16, 17</sup>, Polyacrylonitrile/Epoxy<sup>18</sup>). Although, the presence of thermoplastic content in the resulting fibers can deteriorate their mechanical properties, especially under elevated thermal conditions. The removal of the sacrificial thermoplastic polymer after electrospinning, in a way that does not adversely influence the properties of the resin, has represented a nearly impossible challenge. However, the innovative proposed

1  
2  
3 approach is specifically developed to increase the spinnability of a widely used commercial thermosetting  
4 polymer to produce nanofibers that do not require destructive post-processing.  
5  
6

7 The overarching goal of this work is to create fibers that could be electrospun along with nano  
8 reinforcements such as carbon nanotubes (CNTs) to produce nano hybrid fibril nanocomposites with  
9 enormous surface area as well as surface compatibility to be used with epoxy matrices in advanced  
10 diversified composite applications <sup>19-23</sup>. The degree of dispersion of the nanoparticles into the polymer  
11 matrix always influences the electro-mechanical characteristics of the final products <sup>24, 25</sup>. Accordingly,  
12 CNT is one of the best candidates to make nanocomposites, due to its extraordinary mechanical properties,  
13 <sup>26-29</sup>. Although CNT-based nanocomposites have been developed for many consumer and industrial  
14 products (such as Babolat tennis racquets, Baltic Yacht) <sup>30-32</sup>, major limitations prevent large scale industrial  
15 manufacturing. Most of these nanocomposites are made by an extensive amount of CNT (not a cost-  
16 effective approach <sup>33</sup>). In addition, the lack of good CNT dispersion shows an unexpectedly large increase  
17 in the viscosity of epoxy resins <sup>34</sup>. Industry graded thermosetting epoxy nanocomposites with mechanically  
18 dispersed multi-walled carbon nanotubes have been studied previously <sup>35,36</sup>.  
19  
20  
21  
22  
23  
24  
25

26 Due to the need for making CNT/epoxy based nanocomposite, different researches have been conducted to  
27 make a uniform composite structure. The low dispersion of CNT inside the epoxy structure results in the  
28 formation of clusters due to the Van der Waals forces <sup>37</sup>. The lack of uniform dispersion of CNT inside the  
29 epoxy results in the reduction of mechanical properties of the composite. Recently there have been multiple  
30 researches on making uniform CNT/epoxy structures. As it was reported by Roy et al, using functionalized  
31 CNT can improve the uniformity of the nanocomposite. Carboxylation of the CNT improves the surface  
32 potential of the nanofiber and makes it more soluble in epoxy solvents <sup>38</sup>. Functionalization might reduce  
33 the properties of the CNT so using a physical mixing is more desired to make CNT/epoxy structures <sup>39</sup>.  
34 Multiple methods have been used to develop a well-mixed CNT/epoxy solution such as high-speed steering,  
35 mechanical mixing, roller mixers, ultrasonic radiation and a mixture of these methods. As it was reported  
36 by Barra et al, applying mechanical and ultrasound mixing is the best method of making uniform separation  
37 of CNT inside an epoxy structure <sup>37</sup>. In using this combined method, the CNT will be separated uniformly  
38 inside the structure by mechanical steering while sonication helps the separation of clusters. The byproduct  
39 of this sonication is large amount of heat which is not suitable for the epoxy hardener solution. While the  
40 presence of heat solidifies the epoxy/hardener mixture, perfect timing and combination is needed to mix  
41 CNT in epoxy hardener solutions. Still, to date, controlled dispersion of CNTs for electrospinning have  
42 remained a challenge mostly for a thermosetting polymer matrix such as epoxy. This is due to the Van der  
43 Waals binding energies related to the CNT aggregates, creating clusters and nonuniform network inside the  
44 polymer. Thus, a method is needed to separate the fibers to prevent clustering and make the uniform  
45  
46  
47  
48  
49  
50  
51  
52  
53  
54  
55  
56  
57

1  
2  
3 formation of CNT inside the structure. As it was previously reported, the CNT polymer matrix has been  
4 developed using thermoplastic polymers through an electrospinning process to achieve unidirectional CNT  
5 structures while not adversely impacting the weight of the composite<sup>40</sup>. Despite multiple researches on the  
6 fabrication of CNT composite nanofibers using thermoplastics polymers through an electrospinning  
7 process, there has been no significant research on using thermosetting polymers<sup>40-42</sup>. Due to high viscosity  
8 of thermosetting polymers, adding any nanomaterials such as carbon nanotubes can generate clusters in the  
9 structure, reducing the uniformity and making it less suitable for electrospinning. In this paper, we present  
10 a uniform dispersion of CNT in epoxy polymer that utilizes a multi-step mixing strategy. Here, based on  
11 forced extrusion of CNT-epoxy nanocomposite followed by electrospinning, unidirectional alignment of  
12 carbon nanotubes within electrospun epoxy nanofibers was achieved.

13  
14  
15  
16  
17  
18  
19  
20 Solution parameters (e.g., polymer concentration, viscosity, conductivity, and surface tension) as well as  
21 process parameters (e.g., applied voltage, distance between the capillary tip and collector, and flow rate of  
22 the polymer solution) and ambient parameters (temperature and humidity)<sup>43-46</sup> have been carefully  
23 considered to optimize the sensitized nanofiber morphology. This work shows how to obtain CNT-based  
24 epoxy nanofibers to achieve greater mechanical characteristics in a simple and cost-effective way from an  
25 industrial perspective. Our method for CNT dispersion and nanofiber formation via electrospinning is easily  
26 scalable to higher manufacturing readiness levels.

### 31 **Materials and methods:**

32  
33  
34 A masterbatch of non-functionalized CNTs was used as nano-reinforcements to be mixed with epoxy. The  
35 masterbatch consists of epoxy resin based on Bisphenol A (50 - 99 pbw. %), ethanol solvent (< 15 %  
36 volume) and carbon nanotubes (5 wt. %). The diameter of the nanotubes is in the range of 5-50 nm, with  
37 lengths in the 2-3  $\mu\text{m}$  range. The nano-reinforcement via masterbatch was chosen to avoid CNTs suspension  
38 and to facilitate the dispersion process. Additionally, Dimethylformamide (DMF) and Triton X- 100 were  
39 also effective at separating and suspending carbon nanotubes. Epikure 3234 (triethylenetetramine) (Miller-  
40 Stephenson, USA) was used as the curing agent and was supplied by Hexion specialty chemicals. Samples  
41 were prepared by mixing masterbatch and DMF (1:4 volume ratio) for 10 min using a magnetic stirrer (600  
42 rpm), followed by probe sonication for 10 mins in intervals of 45s and 30s rest between cycles (200W, 20%  
43 Amplitude, 8sec-2sec Pulse). To achieve lower concentration of CNT (2 wt.% and 4 wt.%) the master batch  
44 was mixed with more epoxy. Triton X-100 was then added into the mixture in the ratio of 20:1 and was  
45 stirred for 10 min, followed by sonication in the same manner as before. Neat Epoxy was added in the same  
46 weight as masterbatch and stirred for 15 mins, followed by the same sonication method. The curing agent  
47 was then added to the mixture at a ratio of 15:1 and was allowed to stir at 50°C for 2 hours in order to obtain  
48 a homogeneous solution. The mixture was degassed in a vacuum oven at room temperature for a minimum  
49  
50  
51  
52  
53  
54  
55  
56  
57

of 15 mins and was then allowed to rest for at least 24 hours before electrospinning. Prior to spinning, the prepared solution was added to a syringe with a needle gauge of 26 G. The pumping rate of the epoxy solution was adjusted to 0.5 mL/hr. The electrospinning voltage of 16 kV was applied between the needle and collector at room temperature and a needle tip/collector distance of 10 cm. The collector plate for this experiment was a 20 cm by 20 cm rectangular platinum plate. At a critical voltage (between 12 to 16 kV), a jet of a solution emerged from the needle tip and was accumulated on the collector for 10 mins and stored in a vacuum oven at room temperature for 10 minutes. The process of making submicron CNT/epoxy filaments is shown in figure 1. All the chemical used in the experiments has been provided by Sigma Aldrich, USA, unless it is noted.

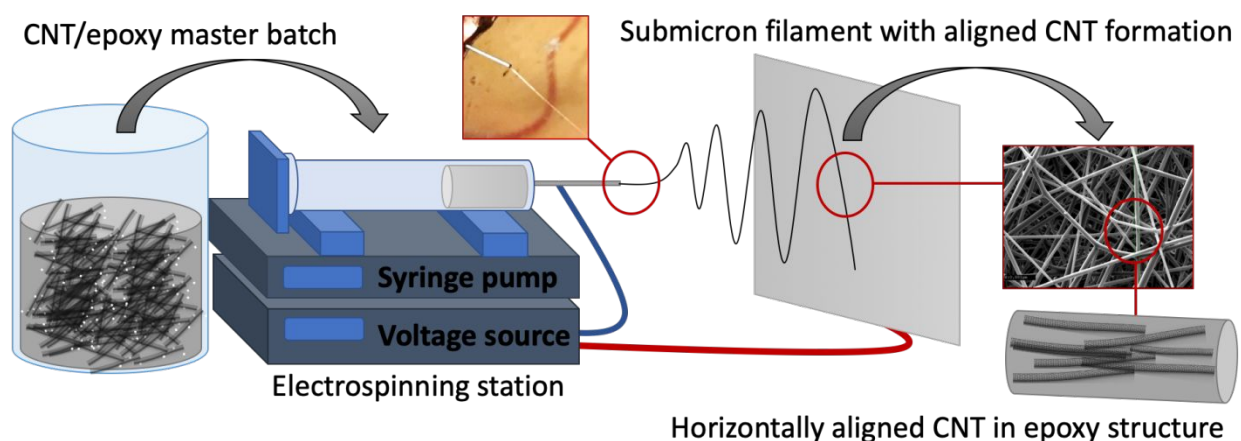


Figure 1 Process schematic for making submicron CNT/epoxy filament through electrospinning

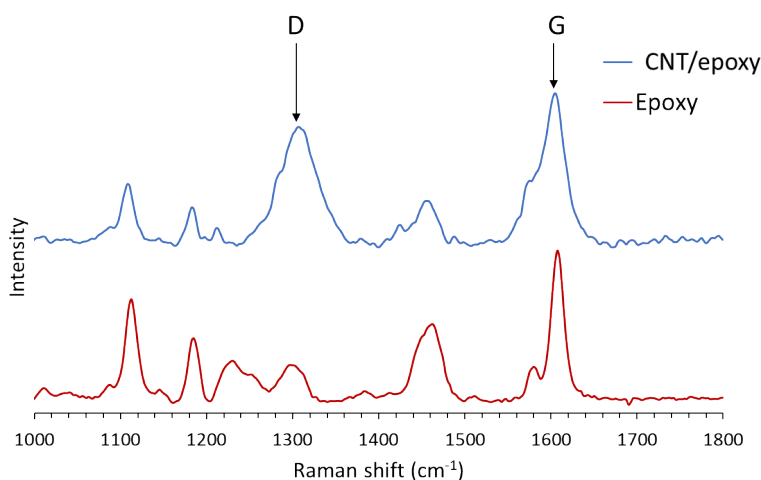
The quality of the fabricated composite was checked using a 785 nm Foster and Freeman Microlaser Raman. Fiber formation and size were analyzed by field emission scanning electron microscopy (FESEM; JEOL 7800F, JEOL Japan). Modulus of the fibers were measured using atomic force microscopy (Bruker, USA). X-ray photoelectron spectroscopy (XPS) and thermal gravimetric analysis (TGA) were conducted with an Omicron XPS/UPS system with argus detector (ScientaOmicron, Germany) and a TA instrument-SDT Q600 TG thermal analyzer (TA, USA). The mechanical properties have been measured using Bruker Catalyst Atomic Force Microscope mounted on a Leica DMI3000 inverted optical microscope (Bruker, USA), and Test Resources 100 Series (Test Resources, USA) according to ASTM D3039 standard.

## Results and discussion:

### CNT/Epoxy Composite:

Morphology and uniformity of the fabricated epoxy composite have been analyzed. The CNT/epoxy batch was observed after preparation and showed no phase separation after 24 hours, and the solution was still

1  
2  
3 dark black after adding the CNT. Further formation of CNT within the epoxy structure after curing was  
4 investigated using Raman Spectroscopy and SEM. A comparison between the Raman spectra of the epoxy  
5 alone and the CNT/epoxy is shown in Figure 2. Raman spectroscopy results revealed that by adding CNT  
6 the peaks for D band 1315 to 1310  $\text{cm}^{-1}$  has been increased, which is related primarily to  $\text{sp}^3$  bonds of  
7 carbon nanotubes, and the G band from 1607 to 1620  $\text{cm}^{-1}$  remains almost constant, which is related to  
8 in-plane sheet  $\text{sp}^2$  hybridized carbon. Here, the presence of D band proves the formation of CNT inside the  
9 epoxy structure. While epoxy is also carbon based, the G band which is related to the  $\text{sp}^2$  hybridization of  
10 carbon in this material. Adding CNT to structure improves the D band shows a change in uniformity of  
11 CNT inside the epoxy structure.  
12  
13  
14  
15  
16  
17  
18  
19



36  
37 *Figure 2 Raman Spectra of a cured CNT/epoxy and Epoxy sample, the D and G bands are*  
38 *marked to reveal the presence of CNT in the structure of composite*

39 SEM analysis revealed that CNT is uniformly mixed within the epoxy solution. In addition, no significant  
40 change in the morphology of the epoxy was observed. This uniform distribution retains the properties of  
41 epoxy while improving its mechanical and electrical properties. The uniform formation of CNT is due to  
42 the presence of DMF, as a polar solvent, and adding plasticizers to prevent clustering. Figure 3(a) shows  
43 SEM image of the resulting CNT/Epoxy sample, where CNT rods were found in the cross-sectional view  
44 of cured CNT-epoxy masterbatch sample. CNT-epoxy fibers showed the uniform formation of randomly  
45 sorted CNT inside the epoxy structure, Figure 3 (b). Higher magnification image figure 3 (c) of the same  
46 structure showed uniformity of the CNT network inside the CNT/epoxy composite. Electrospinning of  
47 2wt.% and 4wt.% CNT-epoxy composites here helped to form unidirectional randomly sorted CNT rods  
48 inside the core of epoxy fibers. It was also realized that by increasing the amount of CNT, at first, the  
49 mixture kept its integrity and uniform structure, but by increasing the weight of CNT to 8 wt.%, clusters of  
50  
51  
52  
53  
54  
55  
56  
57

CNT started to form in the mix. This phenomenon makes the solution made by higher CNT concentration in epoxy, less suitable for electrospinning. Due to this observation, all the samples for this manuscript have been made by 2% and 4% weight of CNT.

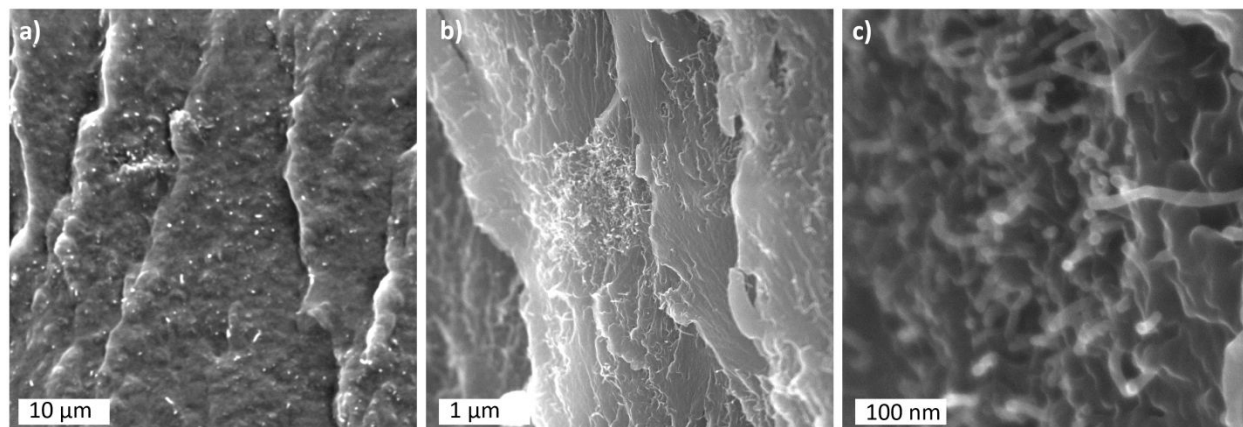


Figure 3 SEM images of cryofractures CNT/epoxy sample revealing a) carbon nanotubes inside CNT-epoxy structure before electrospinning b) the formation of CNTs inside the CNT-epoxy structure and c) uniformity of the CNT network inside the CNT/epoxy composite using higher magnification.

### CNT/Epoxy submicron filaments:

#### *Filament fabrication:*

Rapid change of thermoset resin viscosity makes the fabrication of an electrospun filament challenging, while there is not an added thermoplastic to the solution. To achieve a spinnable viscosity, the epoxy mixture was adjusted using a partial curing method. The partial curing of the thermosetting epoxy helped to achieve enough viscosity to make it spinnable, but not completely cured. Electrospinning is based on the extraction of polyelectrolytes in the form of ionized polymers, thus the Epon epoxy which is based on Bisphenol F, can be ionized and used for electrospinning. The main issue is adding the hardener, which causes instant solidification and makes the epoxy not suitable for electrospinning. Otherwise, removing the hardener also causes structural failure for spun fibers. The epoxy with no hardener is not viscous enough due to the lack of polymer chain formation so it is not spinnable. In this method, adding CNT and partially curing the epoxy/hardener is the key to make submicron fibers through electrospinning. By adding highly conductive CNT nanofibers in the epoxy structure, the ionization of the solution will improve

To check the partial curing process, samples were made with different resting times (5, 20, and 30hrs) and the quality of the resulting fibers was investigated using SEM. Figure 4 shows the change in fiber formation as a result of partial curing resting time. It was found that the lowest resting time (5hrs) was not enough to ensure proper chemical bonding between the epoxy and hardener. Thus, the viscosity is still in the range of



5 p. In contrast, higher rest time (30hrs and more) almost fully cure the epoxy and results in high viscosities in the range of 500 p, preventing the solution to be spinnable. At lower viscosity (i.e. shorter rest time), the filament cannot form because during the electrospinning process, the surface tension of the solution and high electric field produce fragments by entangling the polymer chains. At higher viscosity (i.e. longer rest times) the mixture overcomes the surface tension of the solution and consequently, uniform fibers can be produced. By curing the epoxy solution for too long, higher ratios of entangles affect the uniformity of the fibers and lead to the production of large beads. Moreover, further increasing the curing time results in the solid components (fully cured) that completely damage the uniformity of the filament by hampering the solution flow rate through the needle tip and causing blockages. In this case the 20 hours of resting time is the optimum while the viscosity of the solution reached to 65 p makes it suitable for electrospinning.

Optimization of flow rate is also critical as higher flow rates can cause non-evaporation of the solvent and low stretching of the solution in the jet extruded between the collector and needle tip. These conditions ultimately increase the diameter of the nanofibers and the production of beads and ribbon-like structures<sup>12</sup>. In contrast, low flow rates under the critical point can cause failure in the formation of continuous nanofibers, affecting morphology. Here the flow rates of 0.1 to 1 mL/hr have been investigated. According to the viscosity of the solution, the 0.5 mL/hr flow rate made the best possible fibers. In higher pumping ratios (above 0.7mL/hr) electro spraying starts so instead of having filaments, the uniform layer of CNT/epoxy is achieved, while in lower flow rates (less than 0.4 mL/hr) filaments are not extruding according to the lack of epoxy solution supply.

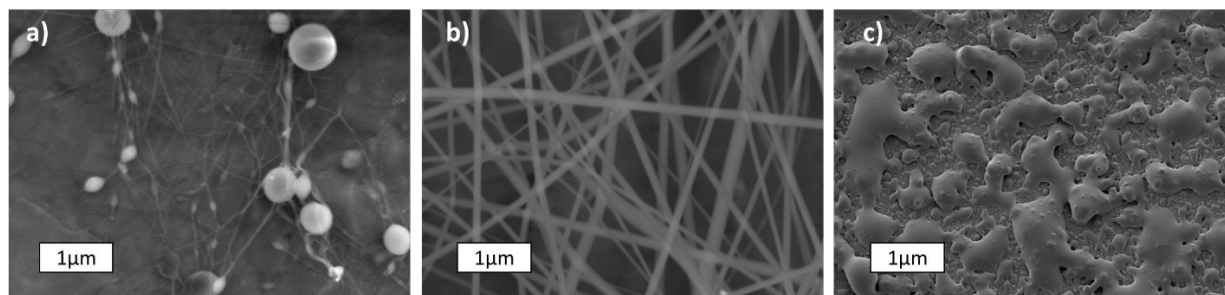
The distance between the needle and the metallic collector also plays a vital role. Several parameters must be optimized considering the deposition time of the polymer solution, the evaporation rate of the solvent, and whipping or instability interval<sup>12,47</sup>. If the distance is kept relatively small, the potential for beaded and large-diameter nanofibers is increased<sup>48</sup>. In this case, 10 cm distance is the optimum. Polymeric concentration with increased viscosity increases the chain entanglement among polymer chains and smooths the formation of continuous nanofibers. Yet, extreme viscosity can completely block the needle tip or start the formation of scattered beaded nanofibers with non-uniform diameters<sup>49</sup>. Figure 4 shows the SEM images of the different electrospun samples that were cured at different times. As is shown here, 20 hours was the best resting time to make submicron filaments. Table 2 shows the settings which were used for each submicron fiber made of specific CNT concentration.

*Table 1 Electrospinning setting parameters for different CNT/epoxy concentrations*

<b>CNT percentage</b>	<b>Cured time (hrs)</b>	<b>Viscosity (p)</b>	<b>Voltage (kV)</b>	<b>Flow rate (mL/hr)</b>	<b>Distance between needle and collector (cm)</b>
0%	20	65	16	0.5	8-10
2%	16	65	16	0.4	9-10



1  
2  
3 4% 15 68 16 0.4 10-10.5  
4  
5  
6



16  
17 *Figure 4 SEM images of electrospun CNT/epoxy solutions after of a) 5 hours, b) 20*  
18 *hours, and c) 30 hours resting time*

19 Surface element compositions of neat epoxy, 2% wt. and 4% wt. MWCNT-epoxy composite electrospun  
20 fibers were analyzed by XPS spectra. Every peak is fitted by using standard carbon binding energy where  
21 the principal peaks of neat epoxy and modified epoxy have almost similar binding energy. For example the  
22 signature of the hydrocarbon peak ( $-C_xH_y-$ ) has been identified for all epoxy type (Figure 5 a,b,c) at the  
23 binding energy of 284.6 eV which is attributed to  $sp^2$ -hybridized graphite-like carbon atoms and  $sp^2$  carbon  
24 atoms bound to hydrogen. But Gaussian peaks for 2% wt. and 4% wt. MWCNT-epoxy are observed  
25 differently. A sharp peak of carbon atoms bound to oxygen atoms by single bond like alkoxy groups (C-O)  
26 starts to form with the binding energy of 286.2 eV<sup>50-52</sup>. for both (Figure 5 b,c) which is originated from  
27  $sp^3$ -hybridized carbon atoms and is similar to that of the diamond-like carbon. A minor peak at 287.3 eV is  
28 observed as well, which is assumed to be carbon atoms bounds with oxygen by a double bond (C=O). Here  
29 the analysis also demonstrates that by adding CNT the formation of alkoxy groups becomes more dominant,  
30 and this can result in having stronger bonding between polymer chains inside the structure. The results  
31 indicate that adding more CNT renders in a higher count of the C-O/C=O bonding and formation of a more  
32 chemically and mechanically stable polymer<sup>51,53</sup>.  
33  
34  
35  
36  
37  
38  
39  
40  
41  
42  
43  
44  
45  
46  
47  
48  
49  
50  
51  
52  
53  
54  
55  
56  
57  
58  
59  
60

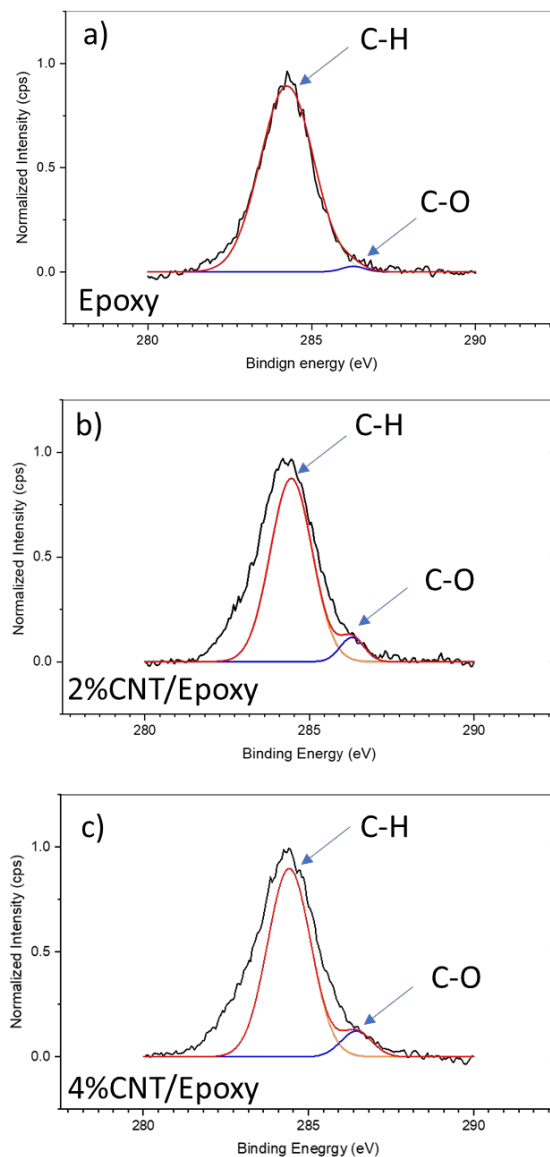


Figure 5 X-ray photoelectron spectroscopy spectra of epoxy composite a) with no, b) with 2% and c) with 4% CNT, the results showing the formation of higher number of C-O bonding by increasing the CNT concentration improving the crystalline structure of the composite

Figure 6 shows the cross-section and top view SEM image of fabricated submicron fibers respectively. As it is noted in figure 6(a), the deposited nanocomposite structure provides a highly porous layer. The thickness of this layer is adjustable by setting spinning parameters and time of electrospinning. The actual size of the fibers was found to be in the range of 100-500 nm along with a uniform distribution. Further, a high magnification cross-section revealed that the CNT nanofibers were unidirectionally embedded inside the epoxy structure. This formation is well-suited for many applications spanning sensors, reinforcements, and different membranes<sup>54, 55</sup>. This formation is due to the applied electric field throughout the electrospinning process. The high electric field moves the direction of the highly conductive CNT rods

1  
2  
3 while the epoxy solution is still not fully cured. Later by extrusion of the filament, the outer shell of the  
4 filament begins to dry and retain the CNT formation in one direction. Another identification from SEM  
5 images is that by increasing the amount of CNT in epoxy mixture the fibers become thinner resulting in  
6 more stiffer fibers. Figures 6(b, c, and d) show the top view of neat epoxy, 2 wt.% CNT/epoxy and 4 wt.%  
7 CNT/epoxy respectively. The identification of the images reveals that the fibers become thinner by  
8 increasing the amount of CNT. The stronger fibers can be stretched more and make thinner filaments  
9 through the electrospinning process. The histogram of each batch has also been provided in figure 6(e) to  
10 compare the size and uniformity of the fibers. As it is shown here, the 4% has the smallest average diameter  
11 in the range of 250 nm while the 2% average is close to 350nm and 0% is around. The distributions of the  
12 thicknesses are based on the same pattern, showing the uniform formation of fibers and adjustability of the  
13 method.  
14  
15  
16  
17  
18  
19  
20  
21  
22  
23  
24  
25  
26  
27  
28  
29  
30  
31  
32  
33  
34  
35  
36  
37  
38  
39  
40  
41  
42  
43  
44  
45  
46  
47  
48  
49  
50  
51  
52  
53  
54  
55  
56  
57  
58  
59  
60

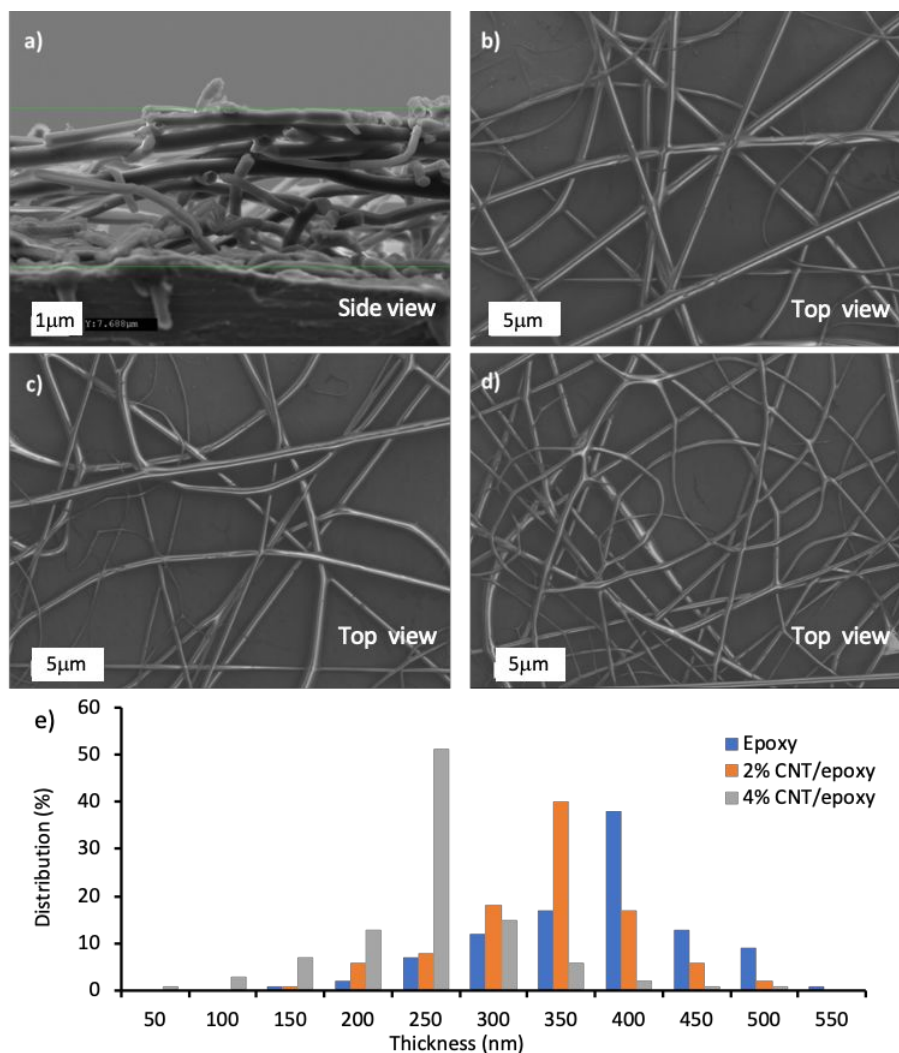
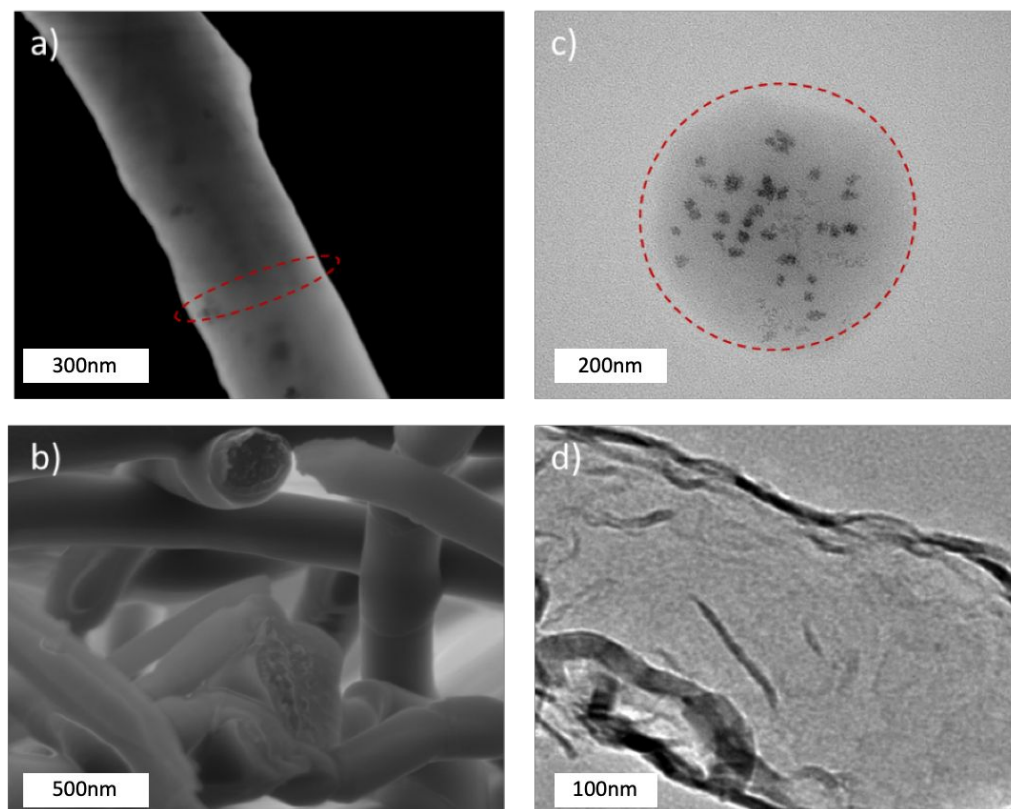


Figure 6 Submicron filaments scaffold a) side view and top view, b) neat epoxy, c) 2 wt.% CNT/epoxy and d) 4 wt.% CNT/epoxy, the uniform formation of the CNT inside the epoxy structure using electrospinning has been shown in the cross section image, e) histogram of fiber size with different CNT concentration

Uniformity of the developed fibers was also observed using STEM and TEM. Figure 7(a) shows a STEM image of the side view of a filament and (b) reveals the cross-section of a filament. The STEM highlights the size of the fibers and the formation of a unidirectional CNT network inside the epoxy structure. Later the side view STEM of the fibers revealed that while CNT rods are made some clusters and some of these rods are bent, but the majority of the clusters and fibers are semi-aligned in the direction of the electric field. As noted in figure 7, the formation of CNT rods inside the filament has been investigated and subsequently, the TEM imaging also proved the formation of the CNT network. Figure 7(c) and (d) show a TEM image of a filament cross-section and side. Here the formation of CNT rods towards the direction of filament has been revealed. It is also observed that this formation is unidirectional due to the presence of

1  
2  
3 an electric field and the electrical conductivity of the CNT network. This network exists while the length  
4 of the CNT is larger than the diameter of the filament the CNT rods in presence of an electric field must be  
5 aligned toward the length of the filaments.  
6  
7

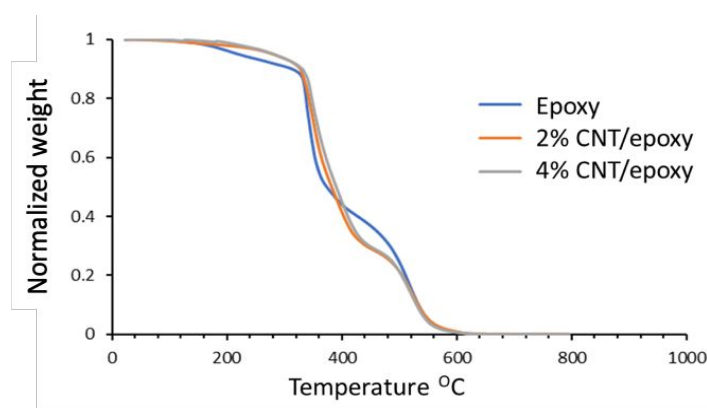


8  
9  
10  
11  
12  
13  
14  
15  
16  
17  
18  
19  
20  
21  
22  
23  
24  
25  
26  
27  
28  
29  
30  
31  
32  
33  
34  
35 *Figure 7 a) top view, b) side view STEM, c) top view and d) side view TEM image of the*  
36 *of the electrospun CNT/epoxy fiber revealing the thickness range, uniformity and*  
37 *unidirectional formation of CNT clusters within the polymer structure*

### 38 *Thermal and mechanical analysis of CNT/epoxy filaments:*

39  
40  
41 Thermal Gravimetric Analysis (TGA) is one of the most widely used methods for investigating polymer  
42 decomposition at different temperatures and thermal stability of materials in general. The thermal stability  
43 of the pristine epoxy, 2 wt.% and 4 wt.% MWCNT-Epoxy filaments was measured at a heating rate of  
44 10°C/min in the presence of nitrogen gas. TGA profile of all these samples showed four steps of degradation  
45 behavior. At first, the neat epoxy experienced initial degradation (around 10% weight loss) at  $T_d \approx 360^\circ\text{C}$   
46 whereas 2 wt.% and 4 wt.% MWCNT-Epoxy composites had similar weight loss at  $\approx 362^\circ\text{C}$  and  $365^\circ\text{C}$ ,  
47 respectively. This small amount of weight loss is attributed to the desorption of physically absorbed water  
48 molecules in the composites<sup>56</sup>. Then in the second step where degradation is maximum (40% weight), neat  
49 epoxy degrades faster than the other two counterparts as scanning temperature reached towards  $400^\circ\text{C}$ .  
50 Possibly since MWNTs are involved in the lower cross-linking degree, decomposition rate of 2 wt.% and  
51  
52  
53  
54  
55  
56  
57  
58  
59  
60

1  
2  
3 4 wt.% MWCNT-Epoxy composites was slower compared to neat epoxy one <sup>57</sup>. Interestingly when the  
4 temperature rose to 520°C, neat epoxy exhibited relatively slow weight decreasing tendency (20% weight).  
5 In the last step (temperature range 520°C to 610°C), all the materials showed similar thermal behavior and  
6 decomposed their rest 30% weight at the same rate. Observing all these curves and their degradation rate at  
7 different temperatures, it has been found that the incorporation of CNTs in the epoxy structure has  
8 effectively increased the thermal stability of epoxy composite structure in a small scale.



14  
15  
16  
17  
18  
19  
20  
21  
22  
23  
24  
25  
26  
27 *Figure 8 Thermal analysis (TGA) of CNT/epoxy filament using different CNT*  
28 *concentration, the thermal analysis reveals the stability of the fibers by adding CNT*

29  
30 The surface area and mesopore structure of the electrospun epoxy and electrospun CNT/epoxy were  
31 characterized by Brunauer–Emmett–Teller (BET) and N<sub>2</sub> adsorption isotherms using an adsorption  
32 instrument (Autosorb iQ2), respectfully. The nitrogen-adsorption and -desorption isotherms and the pore  
33 size distribution of the as-prepared Epoxy with 2% wt nanocarbon content exhibited type V  
34 characteristics as Brunauer has defined which is the most common method used to describe specific  
35 surface area<sup>58, 59</sup>, which are indicative of the presence of mesopores in the composites. The measured  
36 surface area of the neat epoxy was found to be 219 m<sup>2</sup>/g compared to a higher area of 304 m<sup>2</sup>/g for 2 wt.%  
37 MWCNT/epoxy nanofiber. It was confirmed by SEM analysis that adding CNT will increase the surface  
38 area by reducing the fiber diameter. The Barret–Joyner–Halenda (BJH) analyses reveal that for a 2 wt. %  
39 CNT/epoxy porosity is in the range of 5-100nm. This higher surface area makes the developed filaments  
40 suitable for interfacial bonding layers.  
41  
42  
43  
44  
45  
46

47  
48 Figure 9 reveals the improvement of the modulus of the fabricated fibers with the increase of CNT  
49 content measured using atomic force microscopy (Bruker Catalyst Atomic Force Microscope). The test  
50 was carried out based on cantilever deflection method. The transverse compression load deformation of  
51 the filaments was measured by a rectangular MDNISP-HS (Bruker, USA) tip with length of 350 μm and  
52 maximum spring constant of 600 N/m and then used to calculate the modulus of the filament. As it is  
53 shown here, by adding more CNT to the fibers, the mechanical properties have been improved. The  
54  
55  
56  
57

modulus has been increased linearly by increasing the carbon nanotube content. The measured modulus for neat epoxy is 3.24 GPa which is in the range of the reported value from the manufacturer while adding 2% and 4% of CNT has increased this value up to 4.2 GPa and 4.84 GPa, respectively. Here the presence of CNT can lead up to 49% improvement on modulus. As it is shown here, the observed values are in confinement with the rule of mixture, validating the measured results. To validate the measured results, rule of mixture based on the volume concentration and modulus for both CNT and epoxy has been used to predict the modulus of each composite. This can lead to a noticeable improvement of mechanical stability of the fabricated composites using these fibers as reinforcement layers, making them suitable for many applications such as aerospace and energy applications.

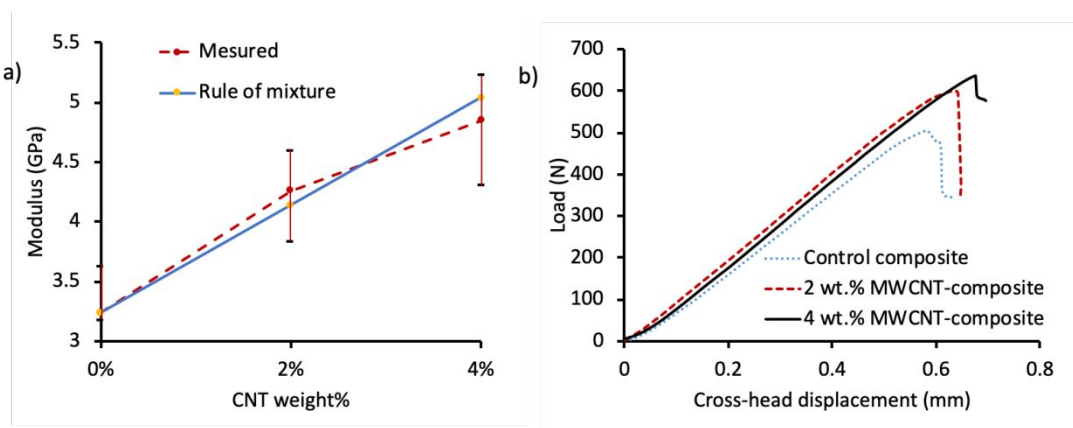


Figure 9 a) Modulus and weight fraction relation of the CNT/epoxy nanofiber with different CNT concentrations, the observed values are in confinement with the rule of mixture, validating the measured results, b) The load-displacement curves of the panels with and without intralayer CNT/epoxy submicron filament reinforcement under flexural loading

To check the quality of the fabricated submicron filament as a reinforcement for carbon fiber reinforced polymer (CFRP) prepreg composites. Thus, the layer of CNT/epoxy filaments has been deposited over a prepreg sheet and then stacked to make a panel. The final panel has 8 layers of prepreg and 7 layers of CNT/epoxy filament sandwiched between layers. As a control a panel with no CNT/epoxy filament has also been made. The Short beam shear strength testing was conducted using ASTM 2344D / M standard, load cell of 2.2 kN and sample size of 2mm×4mm×12mm and a tolerance of 0.01mm. figure 9(b) reveals the load-displacement analysis of both CNT/epoxy and control panels. Here the load values show that the integration on CNT/epoxy filaments improved the strength of the panels by up 19% and 22% by adding reinforcement layer of 2 and 4 wt.% CNT/epoxy filaments between prepreg layers. Further fatigue test was also carried out with loading of a specimen at 60, 70, 80, 90 and 100 percent of static failure load for both panels. The test proved that the failure resistance has been improved by 100% after adding 4 wt.%



1  
2  
3 CNT/epoxy filaments as the reinforcement layer while the presences of aligned CNT improved the bonding  
4 between layers of prepreg.  
5  
6  
7  
8

## 9 **Conclusion**

10  
11 Here, by electrospinning of a CNT/epoxy composite, submicron thermosetting filaments with embedded  
12 aligned CNT networks have been manufactured. Accordingly, the diameter of the fibers and thickness of  
13 the deposited layers could be precisely controlled using this method. Despite the fact that electrospinning a  
14 thermosetting polymer is still a challenge due to low viscosity of the solution and lack of plasticity, we were  
15 capable of making thermosetting polymers spinnable by developing a partial curing strategy through a  
16 thermal treatment process. Thus, spinnable viscosity and chemical bonding were properly achieved for  
17 electrospinning of the thermosetting polymer. Additionally, the very method helped to maintain the shape  
18 of the fiber; thus, multiple layers of the fibers were stacked uniformly without any interlayer deformation  
19 or diffusion. It was also observed that the addition of the CNT to the epoxy improved the mechanical  
20 modulus of the fibers by 49% while reduced the porosity of the fabricated filaments by up to 25 percent.  
21 The addition of CNT to the epoxy structure increased the mechanical properties of the polymer nanofibers,  
22 making them suitable for many composite applications. The obtained CNT/epoxy composites are promising  
23 for reinforcement of the structural composite parts and components in the aerospace, automotive,  
24 motorsports, and sporting goods due to their superior mechanical properties.  
25  
26  
27  
28  
29  
30  
31  
32  
33

## 34 **Acknowledgment**

35  
36  
37 The authors would like to express their gratitude to the National Science Foundation - Small Business  
38 Technology Transfer (STTR) (#2036490) and National Science Foundation- Major Research  
39 Instrumentation Program by supporting this research (#1229514) for the FESEM. Any opinions, findings,  
40 and conclusions or recommendations expressed in this material are those of the author(s) and do not  
41 necessarily reflect the views of the National Science Foundation. The authors would also like to thank Dr.  
42 Daniel Minner, for his assistance with the instrumentation and proofreading, Reza Moheimani for BTU  
43 analysis and Caroline Miller for TEM images.  
44  
45  
46  
47  
48  
49  
50  
51  
52  
53  
54  
55  
56  
57  
58  
59  
60

## References

1. Wang, Y.; He, J.; Chen, H.; Chen, J.; Zhu, R.; Ma, P.; Towers, A.; Lin, Y.; Gesquiere, A. J.; Wu, S. T. J. A. M., Ultrastable, highly luminescent organic–inorganic perovskite–polymer composite films. **2016**, *28* (48), 10710-10717.
2. Ling, T.; Wang, J. J.; Zhang, H.; Song, S. T.; Zhou, Y. Z.; Zhao, J.; Du, X. W. J. A. M., Freestanding ultrathin metallic nanosheets: Materials, synthesis, and applications. **2015**, *27* (36), 5396-5402.
3. Zhao, R.; Lu, X.; Wang, C. J. C. C., Electrospinning based all-nano composite materials: recent achievements and perspectives. **2018**, *10*, 140-150.
4. Gajanan, K.; Tijare, S. J. M. T. P., Applications of nanomaterials. **2018**, *5* (1), 1093-1096.
5. Vijay Kumar, V.; Ramakrishna, S.; Kong Yoong, J. L.; Esmaeely Neisiany, R.; Surendran, S.; Balaganesan, G. J. M. D.; Communications, P., Electrospun nanofiber interleaving in fiber reinforced composites—Recent trends. **2019**, *1* (1), e24.
6. Demir, M. M.; Horzum, N.; Taşdemirci, A.; Turan, K.; Güden, M. J. A. a. m.; interfaces, Mechanical interlocking between porous electrospun polystyrene fibers and an epoxy matrix. **2014**, *6* (24), 21901-21905.
7. Reneker, D. H.; Yarin, A. L., Electrospinning jets and polymer nanofibers. *Polymer* **2008**, *49* (10), 2387-2425.
8. Wan, Y.-Q.; Guo, Q.; Pan, N. J. I. J. o. N. S.; Simulation, N., Thermo-electro-hydrodynamic model for electrospinning process. **2004**, *5* (1), 5-8.
9. Theron, S. A.; Zussman, E.; Yarin, A. L., Experimental investigation of the governing parameters in the electrospinning of polymer solutions. *Polymer* **2004**, *45* (6), 2017-2030.
10. Aliheidari, N.; Aliahmad, N.; Agarwal, M.; Dalir, H. J. S., Electrospun Nanofibers for Label-Free Sensor Applications. **2019**, *19* (16), 3587.
11. Mitchell, G. R., *Electrospinning: principles, practice and possibilities*. Royal Society of Chemistry: 2015.
12. Teo, W. E.; Ramakrishna, S. J. N., A review on electrospinning design and nanofibre assemblies. **2006**, *17* (14), R89.
13. Bhardwaj, N.; Kundu, S. C., Electrospinning: a fascinating fiber fabrication technique. *Biotechnol Adv* **2010**, *28* (3), 325-47.
14. Huang, Z.-M.; Zhang, Y. Z.; Kotaki, M.; Ramakrishna, S., A review on polymer nanofibers by electrospinning and their applications in nanocomposites. *Composites Science and Technology* **2003**, *63* (15), 2223-2253.
15. Megahed, A.; Zoalfakar, S. H.; Hassan, A. E.; Ali, A. A., A novel polystyrene/epoxy ultra-fine hybrid fabric by electrospinning. *Polymers for Advanced Technologies* **2018**, *29* (1), 517-527.
16. Zhang, F.; Zhang, Z.; Liu, Y.; Cheng, W.; Huang, Y.; Leng, J., Thermosetting epoxy reinforced shape memory composite microfiber membranes: Fabrication, structure and properties. *Composites Part A: Applied Science and Manufacturing* **2015**, *76*, 54-61.
17. Yao, Y.; Wang, J.; Lu, H.; Xu, B.; Fu, Y.; Liu, Y.; Leng, J., Thermosetting epoxy resin/thermoplastic system with combined shape memory and self-healing properties. *Smart Materials and Structures* **2015**, *25* (1), 015021.
18. Neisiany, R. E.; Lee, J. K. Y.; Khorasani, S. N.; Ramakrishna, S., Self-healing and interfacially toughened carbon fibre-epoxy composites based on electrospun core–shell nanofibres. *Journal of Applied Polymer Science* **2017**, *134* (31), 44956.

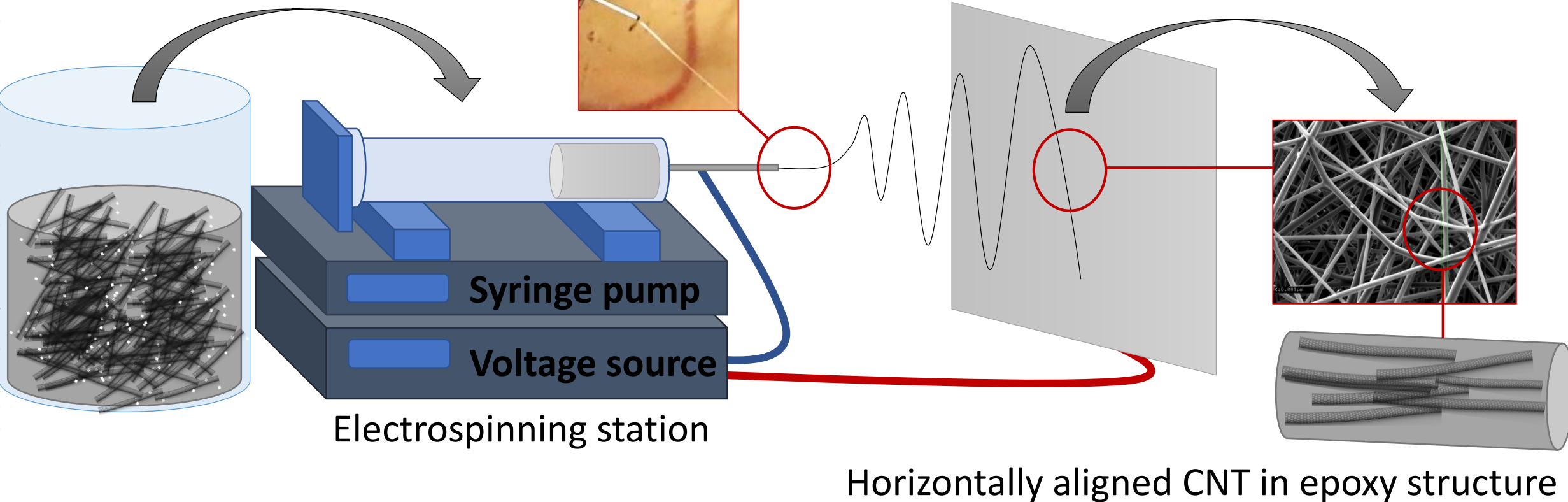
19. Guo, Y.; Yang, X.; Ruan, K.; Kong, J.; Dong, M.; Zhang, J.; Gu, J.; Guo, Z., Reduced graphene oxide heterostructured silver nanoparticles significantly enhanced thermal conductivities in hot-pressed electrospun polyimide nanocomposites. *ACS Applied Materials & Interfaces* **2019**.
20. Wang, Y.; Yang, C.; Pei, Q.-X.; Zhang, Y., Some aspects of thermal transport across the interface between graphene and epoxy in nanocomposites. *ACS applied materials & interfaces* **2016**, *8* (12), 8272-8279.
21. Beckermann, G. W., Nanofiber interleaving veils for improving the performance of composite laminates. *Reinforced Plastics* **2017**, *61* (5), 289-293.
22. Johnsen, B.; Kinloch, A.; Mohammed, R.; Taylor, A.; Sprenger, S., Toughening mechanisms of nanoparticle-modified epoxy polymers. *Polymer* **2007**, *48* (2), 530-541.
23. Rosso, P.; Ye, L.; Friedrich, K.; Sprenger, S., A toughened epoxy resin by silica nanoparticle reinforcement. *Journal of Applied Polymer Science* **2006**, *100* (3), 1849-1855.
24. Wang, Q.; Wu, W.; Gong, Z.; Li, W., Flexural progressive failure of carbon/glass interlayer and intralayer hybrid composites. *Materials* **2018**, *11* (4), 619.
25. Kuwata, M.; Hogg, P., Interlaminar toughness of interleaved CFRP using non-woven veils: Part 1. Mode-I testing. *Composites Part A: Applied Science and Manufacturing* **2011**, *42* (10), 1551-1559.
26. Fiedler, B.; Gojny, F. H.; Wichmann, M. H.; Nolte, M. C.; Schulte, K., Fundamental aspects of nano-reinforced composites. *Composites science and technology* **2006**, *66* (16), 3115-3125.
27. Xie, X.-L.; Mai, Y.-W.; Zhou, X.-P., Dispersion and alignment of carbon nanotubes in polymer matrix: a review. *Materials science and engineering: R: Reports* **2005**, *49* (4), 89-112.
28. Gojny, F. H.; Wichmann, M. H.; Fiedler, B.; Schulte, K., Influence of different carbon nanotubes on the mechanical properties of epoxy matrix composites—a comparative study. *Composites Science and Technology* **2005**, *65* (15-16), 2300-2313.
29. Shaffer, M.; Sandler, J., Carbon nanotube/nanofibre polymer composites. in 'Processing and properties of nanocomposites' (ed.: Advani SG) World Scientific. *New York* **2006**, 1-60.
30. De Volder, M. F.; Tawfick, S. H.; Baughman, R. H.; Hart, A. J., Carbon nanotubes: present and future commercial applications. *science* **2013**, *339* (6119), 535-539.
31. Hussain, F.; Hojjati, M.; Okamoto, M.; Gorga, R. E., Polymer-matrix nanocomposites, processing, manufacturing, and application: an overview. *Journal of composite materials* **2006**, *40* (17), 1511-1575.
32. Aitken, R. J.; Chaudhry, M.; Boxall, A.; Hull, M., Manufacture and use of nanomaterials: current status in the UK and global trends. *Occupational medicine* **2006**, *56* (5), 300-306.
33. Ma, P.-C.; Siddiqui, N. A.; Marom, G.; Kim, J.-K., Dispersion and functionalization of carbon nanotubes for polymer-based nanocomposites: a review. *Composites Part A: Applied Science and Manufacturing* **2010**, *41* (10), 1345-1367.
34. Song, Y. S.; Youn, J. R., Influence of dispersion states of carbon nanotubes on physical properties of epoxy nanocomposites. *Carbon* **2005**, *43* (7), 1378-1385.
35. Giovannelli, A.; Di Maio, D.; Scarpa, F. J. M., Industrial-graded epoxy nanocomposites with mechanically dispersed multi-walled carbon nanotubes: static and damping properties. **2017**, *10* (10), 1222.
36. Özden-Yenigün, E.; Menciloğlu, Y. Z.; Papila, M. J. A. a. m.; interfaces, MWCNTs/P (St-co-GMA) composite nanofibers of engineered interface chemistry for epoxy matrix nanocomposites. **2012**, *4* (2), 777-784.
37. Barra, G.; Guadagno, L.; Vertuccio, L.; Simonet, B.; Santos, B.; Zarrelli, M.; Arena, M.; Viscardi, M., Different Methods of Dispersing Carbon Nanotubes in Epoxy Resin and Initial Evaluation of the Obtained Nanocomposite as a Matrix of Carbon Fiber Reinforced Laminate in Terms of Vibroacoustic Performance and Flammability. *Materials (Basel, Switzerland)* **2019**, *12* (18), 2998.
38. Roy, S.; Petrova, R. S.; Mitra, S., Effect of carbon nanotube (CNT) functionalization in Epoxy-CNT composites. *Nanotechnol Rev* **2018**, *7* (6), 475-485.

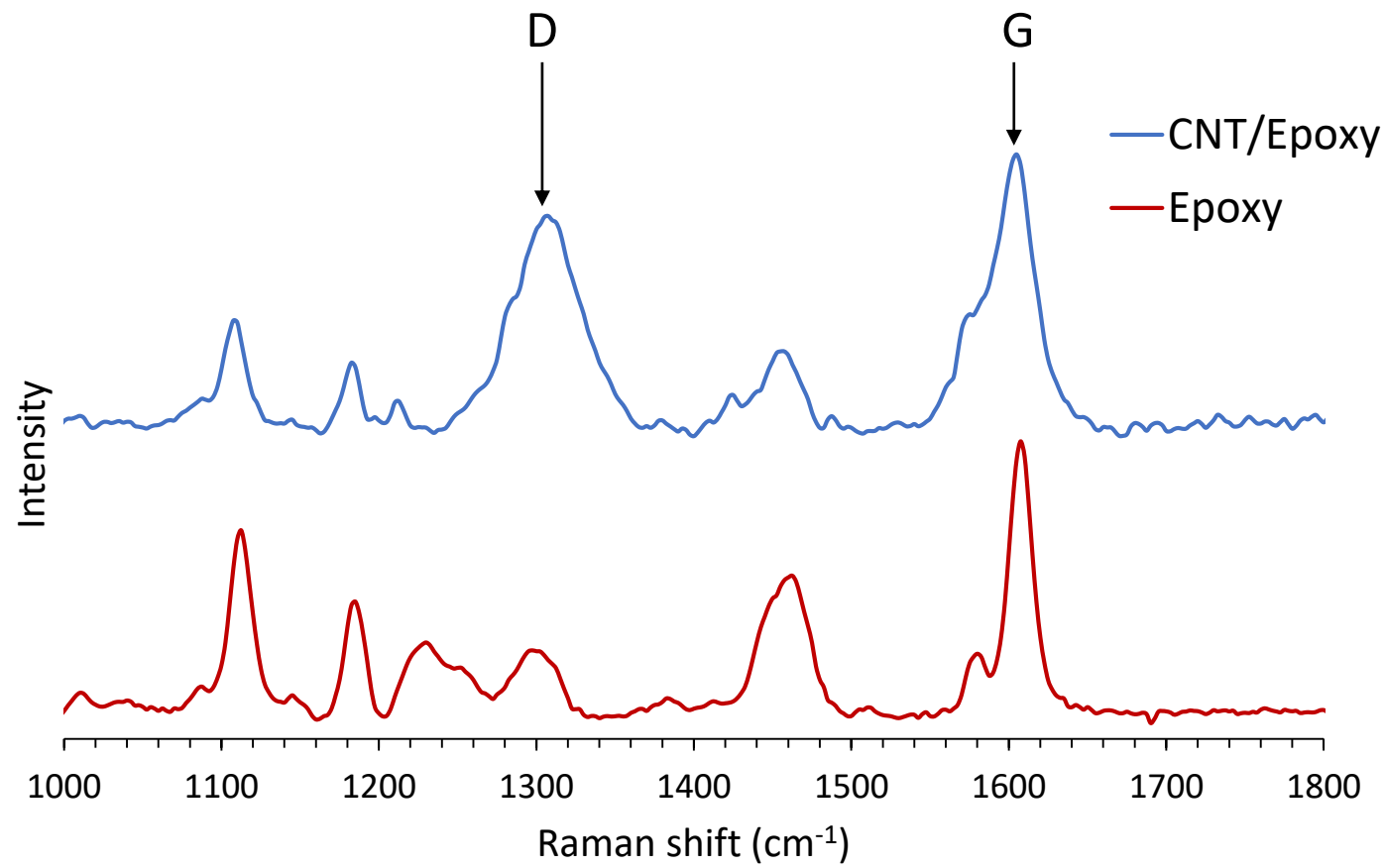
39. Singh, P.; Sharma, K.; Kumar, A.; Shukla, D. M., Effects of functionalization on the mechanical properties of multiwalled carbon nanotubes: A molecular dynamics approach. *Journal of Composite Materials* **2016**, *51*, 671-680.
40. Ko, F.; Gogotsi, Y.; Ali, A.; Naguib, N.; Ye, H.; Yang, G.; Li, C.; Willis, P., Electrospinning of continuous carbon nanotube-filled nanofiber yarns. *Advanced materials* **2003**, *15* (14), 1161-1165.
41. Sen, R.; Zhao, B.; Perea, D.; Itkis, M. E.; Hu, H.; Love, J.; Bekyarova, E.; Haddon, R. C., Preparation of single-walled carbon nanotube reinforced polystyrene and polyurethane nanofibers and membranes by electrospinning. *Nano letters* **2004**, *4* (3), 459-464.
42. Kausar, A., Polyamide-grafted-multi-walled carbon nanotube electrospun nanofibers/epoxy composites. *Fibers and Polymers* **2014**, *15* (12), 2564-2571.
43. Huang, Z.-M.; Zhang, Y.-Z.; Kotaki, M.; Ramakrishna, S., A review on polymer nanofibers by electrospinning and their applications in nanocomposites. *Composites science and technology* **2003**, *63* (15), 2223-2253.
44. Bhardwaj, N.; Kundu, S. C., Electrospinning: a fascinating fiber fabrication technique. *Biotechnology advances* **2010**, *28* (3), 325-347.
45. Thompson, C.; Chase, G. G.; Yarin, A.; Reneker, D., Effects of parameters on nanofiber diameter determined from electrospinning model. *Polymer* **2007**, *48* (23), 6913-6922.
46. Ali, A. A.; Eltabey, M.; Farouk, W.; Zoalfakar, S. H., Electrospun precursor carbon nanofibers optimization by using response surface methodology. *Journal of Electrostatics* **2014**, *72* (6), 462-469.
47. Matabola, K. P.; Moutloali, R. M., The influence of electrospinning parameters on the morphology and diameter of poly(vinylidene fluoride) nanofibers- effect of sodium chloride. *Journal of Materials Science* **2013**, *48* (16), 5475-5482.
48. Zhang, C.; Yuan, X.; Wu, L.; Han, Y.; Sheng, J., Study on morphology of electrospun poly(vinyl alcohol) mats. *European Polymer Journal* **2005**, *41* (3), 423-432.
49. Haider, S.; Al-Zeghayer, Y.; Ahmed Ali, F. A.; Haider, A.; Mahmood, A.; Al-Masry, W. A.; Imran, M.; Aijaz, M. O., Highly aligned narrow diameter chitosan electrospun nanofibers. *Journal of Polymer Research* **2013**, *20* (4).
50. Kettle, J.; Ding, Z.; Horie, M.; Smith, G. J. O. E., XPS analysis of the chemical degradation of PTB7 polymers for organic photovoltaics. **2016**, *39*, 222-228.
51. Williams, T.; Yu, H.; Woo, R.; GRIGORIEV, M.; CHENG, D.; HICKS, R. F. J. A. M. P. L., Atmospheric Pressure Plasma as a Method for Improving Adhesive Bonding. **2014**, *2631*.
52. Daneshkhah, A.; Vij, S.; Siegel, A. P.; Agarwal, M. J. C. E. J., Polyetherimide/carbon black composite sensors demonstrate selective detection of medium-chain aldehydes including nonanal. **2019**, 123104.
53. Zaldivar, R.; Nokes, J.; Steckel, G.; Kim, H.; Morgan, B. J. J. o. c. m., The effect of atmospheric plasma treatment on the chemistry, morphology and resultant bonding behavior of a pan-based carbon fiber-reinforced epoxy composite. **2010**, *44* (2), 137-156.
54. Naebe, M.; Lin, T.; Feng, L.; Dai, L.; Abramson, A.; Prakash, V.; Wang, X., Conducting polymer and polymer/cnt composite nanofibers by electrospinning. ACS Publications: 2009.
55. He, X.-X.; Zheng, J.; Yu, G.-F.; You, M.-H.; Yu, M.; Ning, X.; Long, Y.-Z. J. T. J. o. P. C. C., Near-field electrospinning: progress and applications. **2017**, *121* (16), 8663-8678.
56. Riaz, S.; Park, S. J., Thermal and Mechanical Interfacial Behaviors of Graphene Oxide-Reinforced Epoxy Composites Cured by Thermal Latent Catalyst. *Materials (Basel)* **2019**, *12* (8).
57. Damian, C.; Pandele, A.; Iovu, H., Ethylenediamine functionalization effect on the thermo-mechanical properties of epoxy nanocomposites reinforced with multiwall carbon nanotubes. *UPB Scientific Bulletin, Series B: Chemistry and Materials Science* **2010**, *72*.
58. Dollimore, D.; Heal, G., An improved method for the calculation of pore size distribution from adsorption data. *Journal of applied chemistry* **1964**, *14* (3), 109-114.
59. Drake, L., Pore-size distribution in porous materials. *Industrial & Engineering Chemistry* **1949**, *41* (4), 780-785.

1  
2  
3  
4  
5  
6  
7  
8  
9  
10  
11  
12  
13  
14  
15  
16  
17  
18  
19  
20  
21  
22  
23  
24  
25  
26  
27  
28  
29  
30  
31  
32  
33  
34  
35  
36  
37  
38  
39  
40  
41  
42  
43  
44  
45  
46  
47  
48  
49  
50  
51  
52  
53  
54  
55  
56  
57  
58  
59  
60

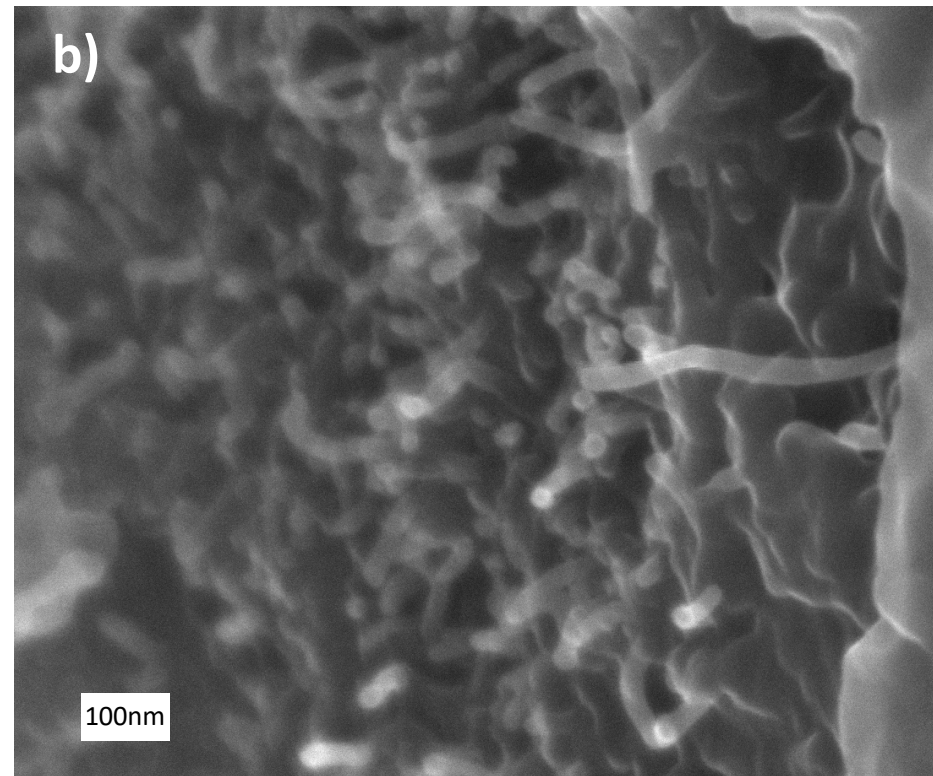
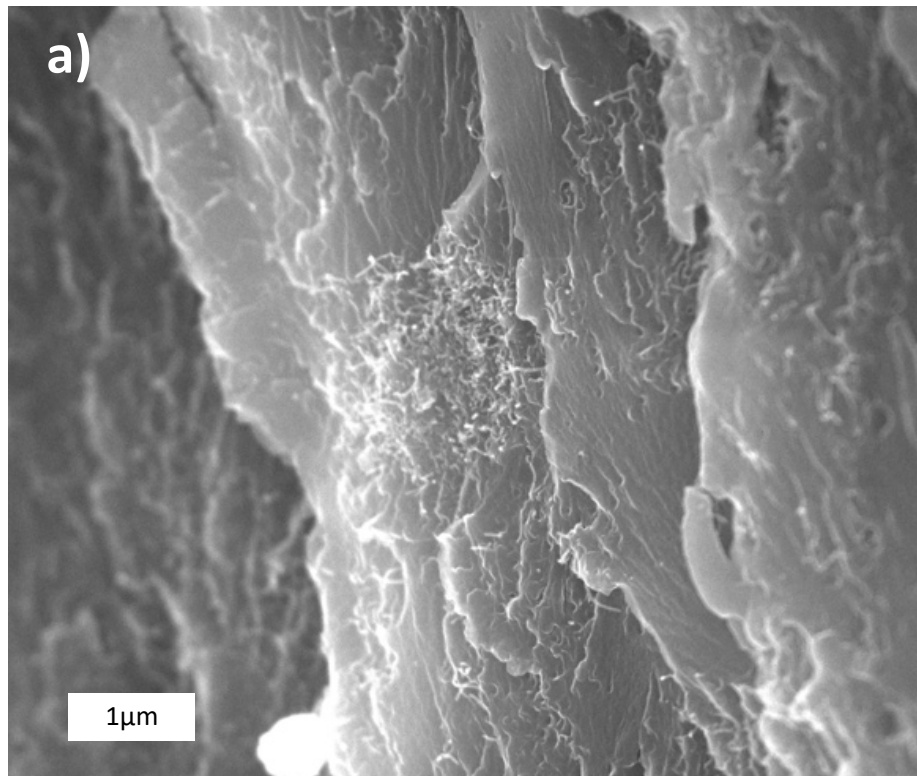
1  
2  
3  
4  
5  
6  
7  
8  
9  
10  
11  
12  
13  
14  
15  
16  
17  
18  
19  
20  
21  
22  
23  
24  
25  
26  
27  
28  
29  
30  
31  
32  
33  
34  
35  
36  
37  
38  
39  
40  
41

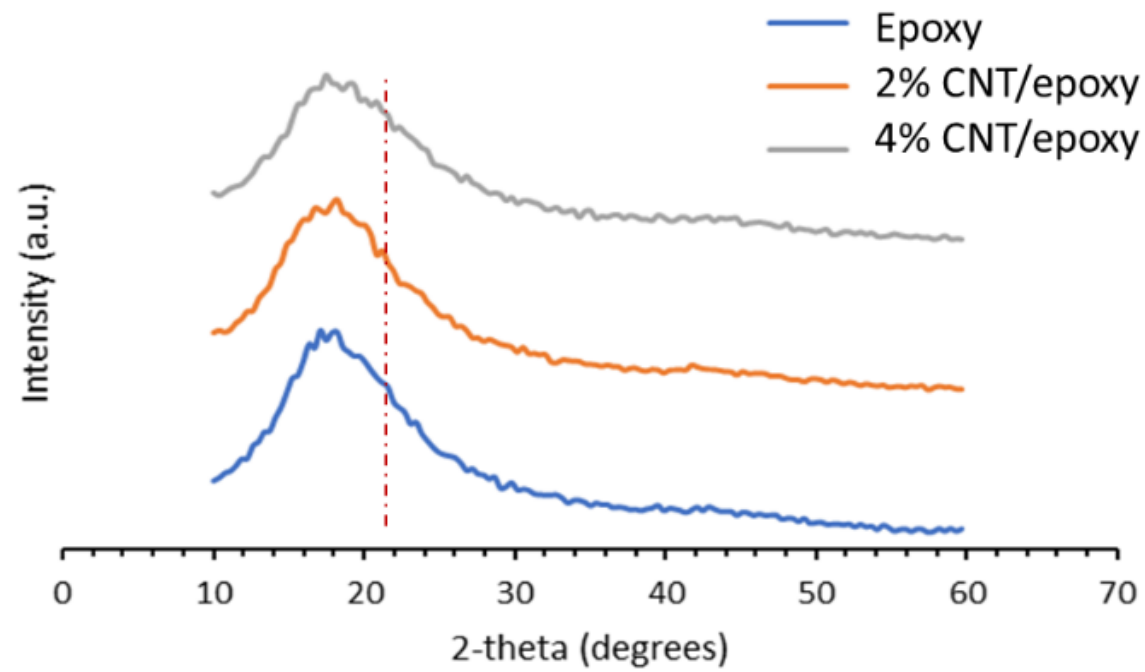
CNT/Epoxy master batch





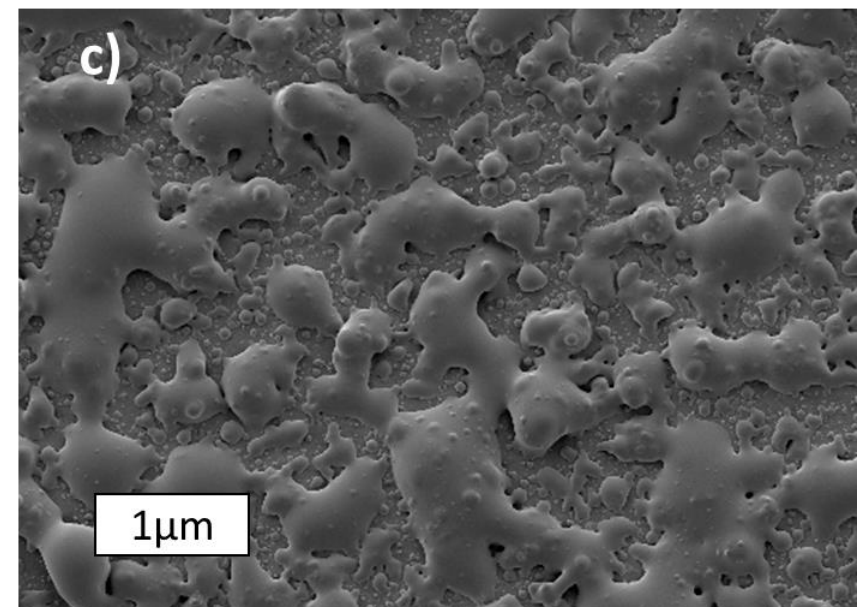
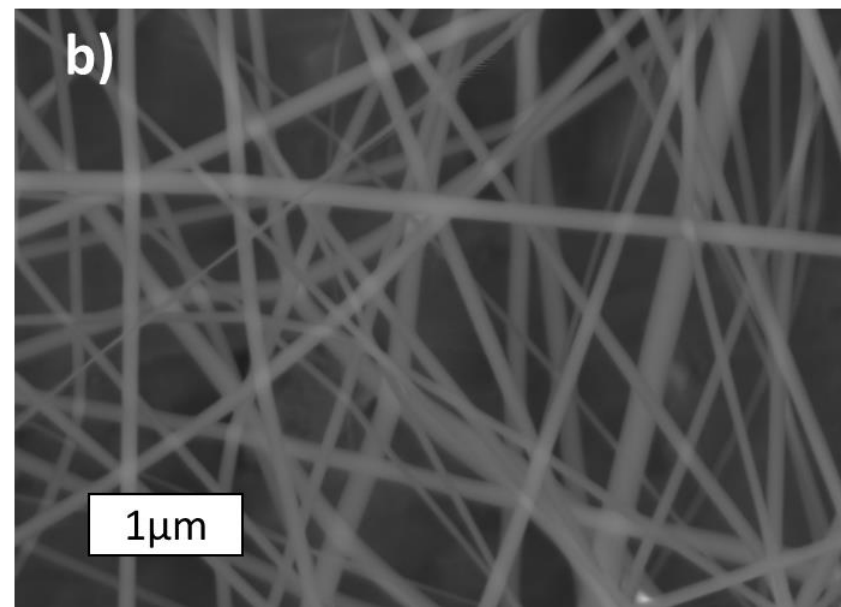
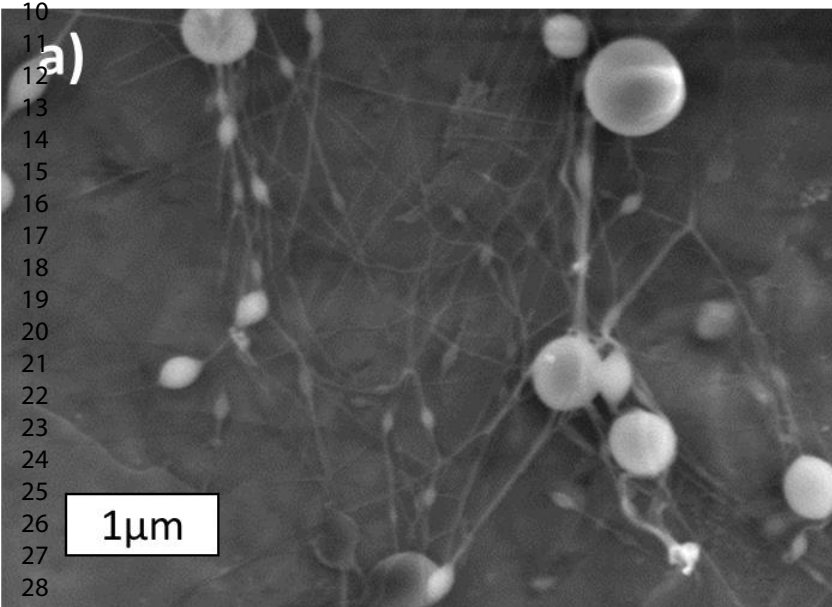




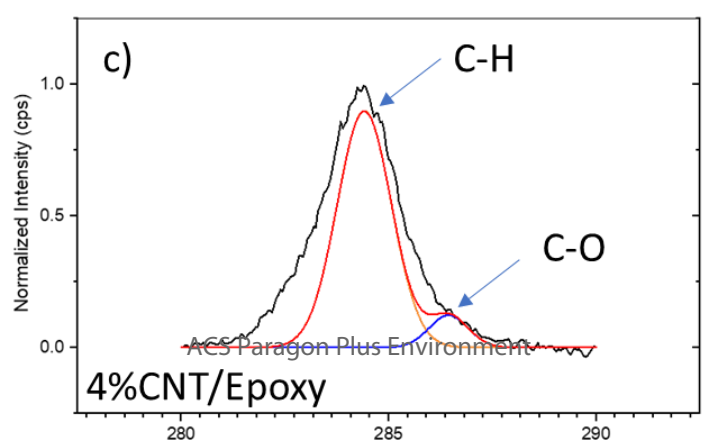
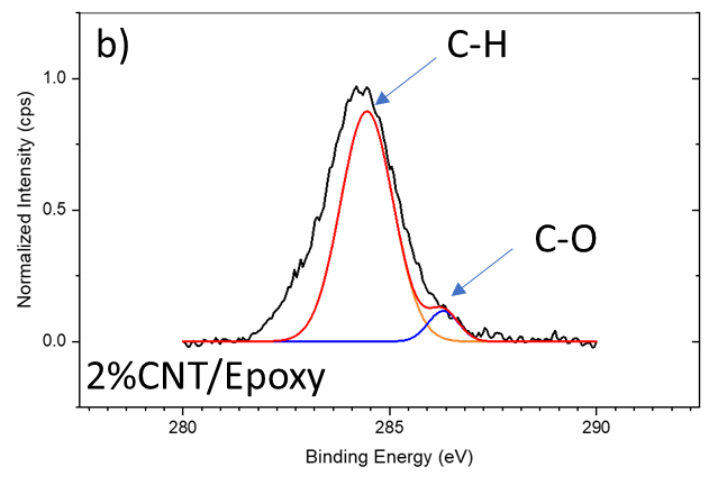
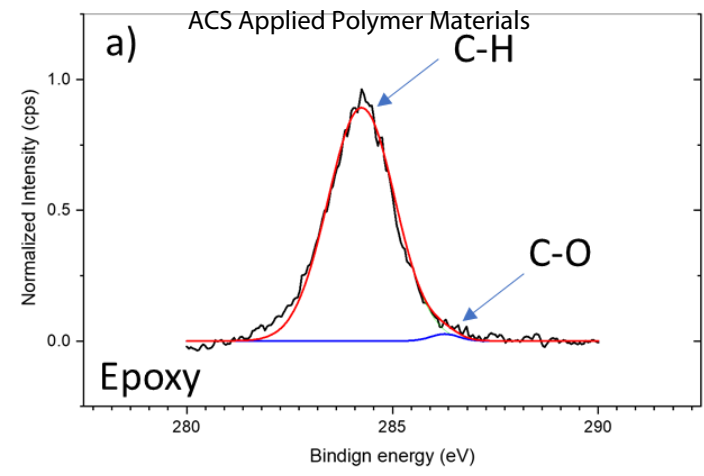


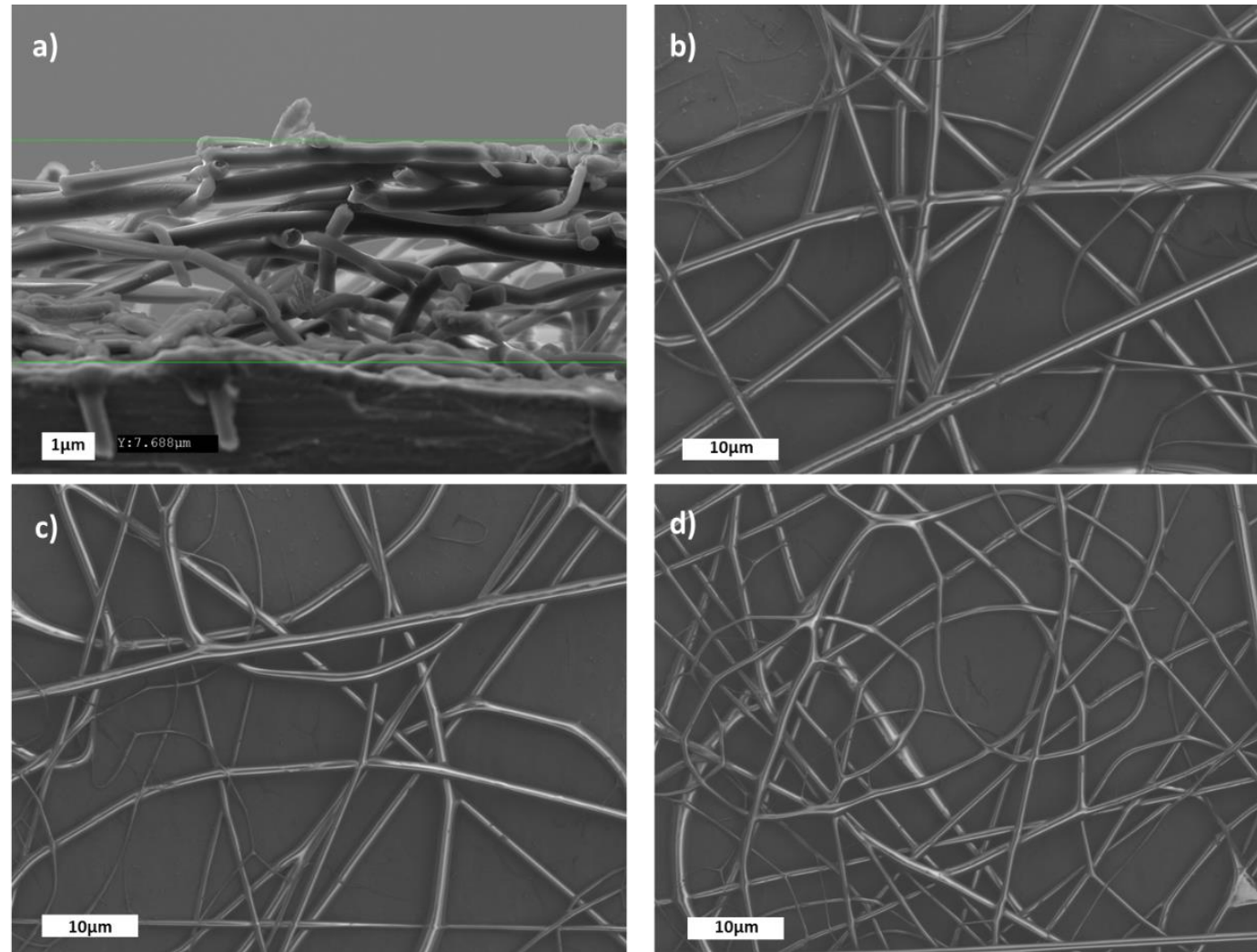
1  
2  
3  
4  
5  
6  
7  
8  
9  
10  
11  
12  
13  
14  
15  
16  
17  
18  
19  
20  
21  
22  
23  
24  
25  
26  
27  
28  
29  
30  
31  
32  
33  
34  
35  
36  
37  
38  
39  
40  
41

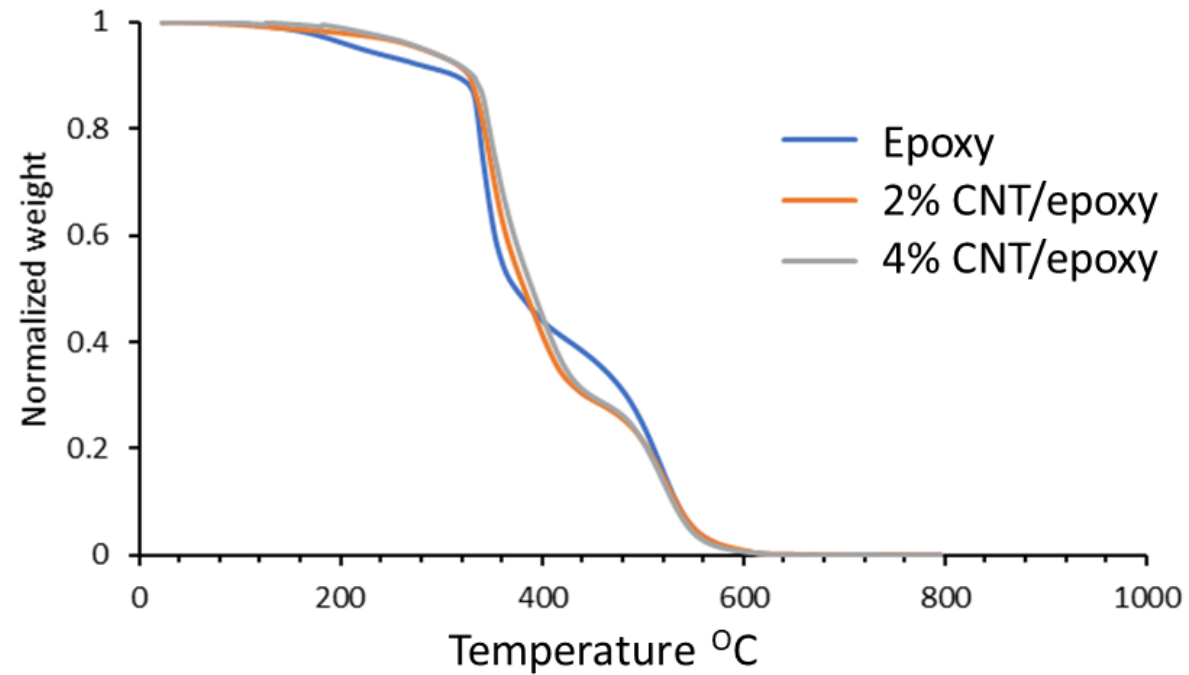
1  
2  
3  
4  
5  
6  
7  
8  
9  
10  
11  
12  
13  
14  
15  
16  
17  
18  
19  
20  
21  
22  
23  
24  
25  
26  
27  
28  
29  
30  
31  
32  
33  
34  
35  
36  
37  
38  
39  
40  
41

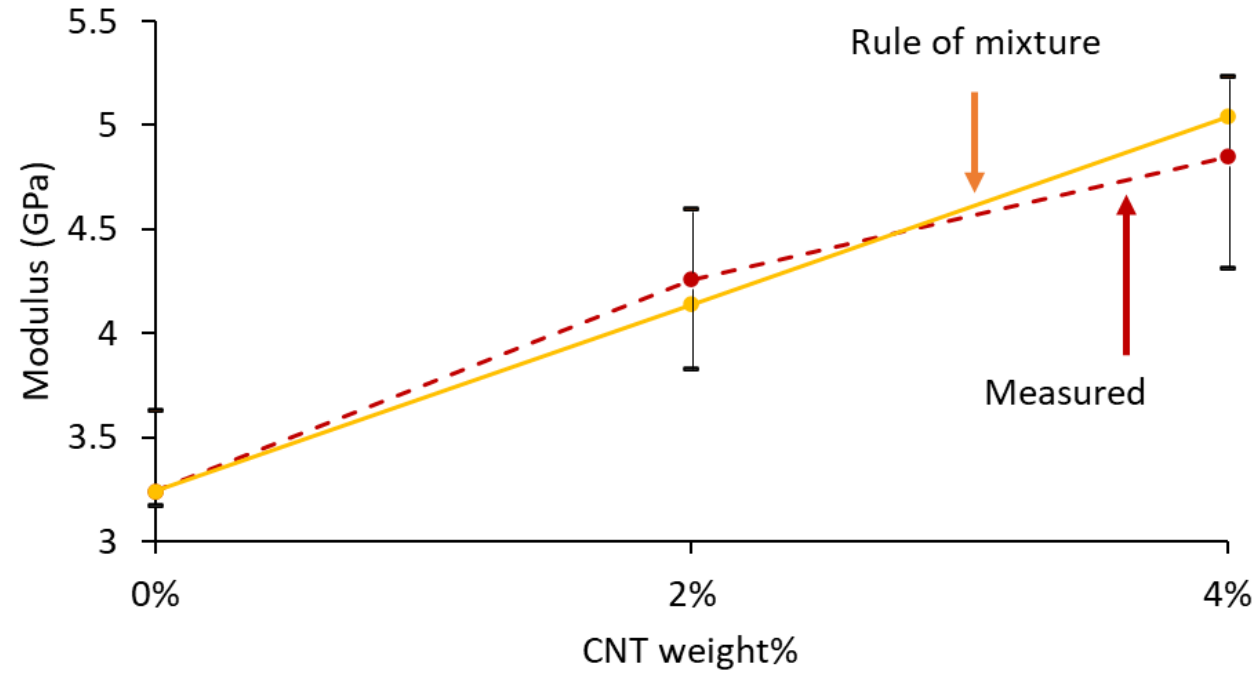


1  
2  
3  
4  
5  
6  
7  
8  
9  
10  
11  
12  
13  
14  
15  
16  
17  
18  
19  
20  
21  
22  
23  
24  
25  
26  
27  
28  
29  
30  
31  
32  
33  
34  
35  
36  
37  
38  
39  
40  
41











1  
2  
3  
4  
5  
6  
7  
8  
9  
10  
11  
12  
13  
14  
15  
16  
17  
18  
19  
20  
21  
22  
23  
24  
25  
26  
27  
28  
29  
30  
31  
32  
33  
34  
35  
36  
37  
38  
39  
40  
41

